PROCEEDINGS B

royalsocietypublishing.org/journal/rspb

Research





Cite this article: Mongiardino Koch N, Tilic E, Miller AK, Stiller J, Rouse GW. 2023 Confusion will be my epitaph: genome-scale discordance stifles phylogenetic resolution of Holothuroidea. *Proc. R. Soc. B* **290**: 20230988. https://doi.org/10.1098/rspb.2023.0988

Received: 02 May 2023 Accepted: 12 June 2023

Subject Category:

Evolution

Subject Areas:

evolution, genomics, taxonomy and systematics

Keywords:

sea cucumbers, systematics, phylogenomics, phylogenetic signal, phylogenetic conflict

Author for correspondence:

Nicolás Mongiardino Koch

e-mail: nmongiardinokoch@ucsd.edu

Electronic supplementary material is available online at https://doi.org/10.6084/m9.figshare. c.6707571.

THE ROYAL SOCIETY

Confusion will be my epitaph: genomescale discordance stifles phylogenetic resolution of Holothuroidea

Nicolás Mongiardino Koch¹, Ekin Tilic^{1,2}, Allison K. Miller³, Josefin Stiller⁴ and Greg W. Rouse¹

NMK, 0000-0001-6317-5869

Sea cucumbers (Holothuroidea) are a diverse clade of echinoderms found from intertidal waters to the bottom of the deepest oceanic trenches. Their reduced skeletons and limited number of phylogenetically informative traits have long obfuscated morphological classifications. Sanger-sequenced molecular datasets have also failed to constrain the position of major lineages. Noteworthy, topological uncertainty has hindered a resolution for Neoholothuriida, a highly diverse clade of Permo-Triassic age. We perform the first phylogenomic analysis of Holothuroidea, combining existing datasets with 13 novel transcriptomes. Using a highly curated dataset of 1100 orthologues, our efforts recapitulate previous results, struggling to resolve interrelationships among neoholothuriid clades. Three approaches to phylogenetic reconstruction (concatenation under both site-homogeneous and site-heterogeneous models, and coalescent-aware inference) result in alternative resolutions, all of which are recovered with strong support and across a range of datasets filtered for phylogenetic usefulness. We explore this intriguing result using gene-wise log-likelihood scores and attempt to correlate these with a large set of gene properties. While presenting novel ways of exploring and visualizing support for alternative trees, we are unable to discover significant predictors of topological preference, and our efforts fail to favour one topology. Neoholothuriid genomes seem to retain an amalgam of signals derived from multiple phylogenetic histories.

1. Introduction

Holothuroidea (commonly known as sea cucumbers) is arguably the most morphologically diverse major clade of extant Echinodermata (figure 1). The smallest adults can be less than 1 cm in length, as seen in the meiofaunal *Leptosynapta minuta* [1] and epibenthic *Incubocnus* [2]. The largest can be thin and elongate, reaching several metres length, as in the snake sea cucumber *Synapta maculata* [3], or they may be less than a metre but robust and weighing over 5 kg, as in the case of *Holothuria fuscopunctata* [4]. While predominantly benthic as adults, some taxa are capable of swimming and there are even forms that spend their entire lives in the water column, as *Pelagothuria natatrix* does [5]. While all holothuroids have a ring of tentacles and are deposit or filter feeders, some clades lack tube feet and have a substantially reduced water vascular system, traits otherwise developed across all echinoderms. They can also entirely lack calcareous elements (ossicles) in the body wall, or these can be expanded to form overlapping plates that build a rigid test [6]. There are currently 1775 accepted extant species of holothuroids [7] found in ocean waters that range from the

© 2023 The Authors. Published by the Royal Society under the terms of the Creative Commons Attribution License http://creativecommons.org/licenses/by/4.0/, which permits unrestricted use, provided the original author and source are credited.

¹Scripps Institution of Oceanography, University of California San Diego, La Jolla, CA, USA

²Department of Marine Zoology, Senckenberg Research Institute and Museum, Frankfurt, Germany

³Anatomy Department, University of Otago, Dunedin, Otago, New Zealand

⁴Centre for Biodiversity Genomics, Section for Ecology and Evolution, Department of Biology, University of Copenhagen, Copenhagen, Denmark



Figure 1. Representative holothuroid diversity included in this study. (a). Synapta sp. (b). Peniagone cf. vitrea. (c). Benthogone sp. (d). Pseudocolochirus violaceus. (e). Abyssocucumis albatrossi. (f). Colochirus robustus. (g). Ypsilothuria n. sp. (SIO-BIC E6221). (h). Molpadia amorpha. (i). Pseudostichopus cf. mollis. (j). Synallactidae. (k). Bathyplotes cf. moseleyi. The classification of these terminals can be found in electronic supplementary material, table S1. All photos except (g) are of the voucher specimens sequenced (catalogue numbers can be found in electronic supplementary material, table S1; further sampling information is accessible through the SIO-BIC online database, https://sioapps.ucsd.edu/collections/bi/). Images (b), (c), (i) and (k) are courtesy of the Schmidt Ocean Institute, and image (j) is courtesy of Monterey Bay Aquarium and Research Institute.

intertidal to the bottom of the deepest trenches [8,9]. Especially in benthic deep-sea habitats, they can constitute the vast majority of total biomass and have a strong impact on ecosystem functioning, bioturbation and nutrient cycling [10–12].

Downloaded from https://royalsocietypublishing.org/ on 01 April 2024

While multiple morphological attempts have been made to delineate major subdivisions within Holothuroidea, these have been limited by the extreme simplification of their skeleton (relative to other echinoderms), the delicate and fragile nature of their bodies (which often results in poorly preserved specimens for morphological analyses) and the small number of traits that provide useful information at high taxonomic levels [13–15]. The most recent revision of the group's

classification was based on a six-gene dataset including terminals from 25 of the 29 accepted family ranked taxa [16]. This study recovered a basal split within sea cucumbers between Apodida, a clade characterized by a complete loss of tube feet, and Actinopoda (among which secondary reductions or loss of tube feet occur only within Molpadida). Actinopoda were further subdivided into Elasipodida and Pneumonophora, the latter of which includes all species with respiratory trees, a unique cloacal invagination that plays an important (although not exclusive) role in respiration [17,18]. Furthermore, the names Holothuriida and Neoholothuriida were applied to the main subdivisions within Pneumonophora, with four well-supported major clades inside Neoholothuriida: Dendrochirotida, Molpadida, Persiculida and Synallactida. However, the relationships among these four lineages remained uncertain. A phylogenetic resolution for the major neoholothuriid lineages is necessary to explore the origins of the high morphological and ecological disparity harboured by this clade, as well as to establish a natural classification framework for a substantial fraction of sea cucumber diversity (62% of species-level diversity is contained within Neoholothuriida [7]). Miller et al. [16] concluded that meeting these objectives would likely require sequencing efforts of a different magnitude.

Here we present the first phylogenomic study of sea cucumbers, the last major eleutherozoan clade (which further includes echinoids [19], asteroids [20] and ophiuroids [21]) to have its phylogeny tackled using genome-scale datasets. Through the generation of novel transcriptomic resources for holothuroids we built a molecular dataset encompassing over a thousand orthologues. The goal was to resolve some of the lingering uncertainties in the holothuroid tree of life, yet a continuing lack of resolution encouraged novel ways to explore phylogenomic datasets.

2. Material and methods

(a) Taxon sampling, extraction and sequencing

Sea cucumber specimens were collected by SCUBA diving, snorkeling, dredging and remotely operated vehicles (ROV), or purchased from aquarium suppliers. Specimen collection and fieldwork was performed under permits whenever applicable. All vouchers were deposited at the Benthic Invertebrate Collection, Scripps Institution of Oceanography (SIO-BIC; electronic supplementary material, table S1). Species identification was based on multiple lines of evidence, including anatomical (gross and ossicle morphology), biogeographical and molecular (mitochondrial cytochrome c oxidase subunit I, COI) information. DNA extractions and COI amplifications followed protocols described in Miller et al. [16], and sequences are deposited in NCBI (accession numbers available in electronic supplementary material, table S1). In the case of unavailable COI sequences, these were mined from assembled transcriptomes by blasting against close relatives. identifications of transcriptomic vouchers at SIO were also revised, including those sequenced and released as part of EchinoDB [22,23].

For large specimens, tissue was dissected from the body wall or tube feet, while whole body sections were sampled for the remaining samples. Sampled tissues were finely chopped, placed in RNAlater (Invitrogen) buffer solution, and stored at -80°C. RNA extractions were performed from Trizol (Thermofisher), using Direct-zol RNA Miniprep Kit with in-column DNAse treatment (Zymo Research). mRNA was isolated with Dynabeads mRNA Direct Micro Kit (Invitrogen). mRNA concentration was estimated using Qubit RNA broad range assay kit (Thermofisher), and quality was assessed using RNA ScreenTape with an Agilent 4200 TapeStation on an Agilent Bioanalyzer 2100. Most libraries were prepared using a KAPA-Stranded RNA-Seq kit targeting a 200-300 bp insert size, and results were assessed using DNA ScreenTape (Bioanalyzer 2100). Libraries were then sequenced in multiplexed (8 libraries per lane) pair-end runs using 150 bp paired-end Illumina HiSeq 4000 at the UC San Diego IGM Genomics Center. To minimize read crossover, we employed 10 bp sequence tags designed to be robust to indel and substitution errors [24]. For four samples (Benthodytes cf. sanguinolenta, Benthogone sp., Colochirus robustus and Peniagone cf. vitrea), library preparation and multiplexed pair-end sequencing on an Illumina NovaSeq 6000 PE150 was performed by Novogene.

Thirteen novel transcriptomes were generated for this study and combined with publicly available genomic and transcriptomic datasets downloaded from NCBI and EchinoBase [25]. Final taxonomic sampling included 35 holothuroids as well as three echinoid and one asteroid outgroups (electronic supplementary material, table S1). Raw files for all novel datasets, as well as those so far available only on EchinoDB [22], are deposited in the NCBI sequence read archive (SRA) under BioProject PRJNA979278. All assemblies are available at the associated Dryad data repository (doi:10.5061/dryad.0p2ngf255) [26], along with the phylogenetic matrices, trees and other results derived from them.

(b) Assembly, sanitation and matrix construction

Reads were trimmed or excluded based on quality scores using Trimmomatic v 0.3.6 under default settings [27]. Additional sanitation steps were implemented by the Agalma 2.0 pipeline [28], resulting in the removal of reads based on compositional and quality filtering criteria, as well as those mapping to rRNA sequences or retaining adapter sequences. Remaining reads were assembled de novo with Trinity v. 2.5.1 [29]. Assemblies were then screened for contaminants using alien_index v 3.0 [30]. Transcripts with substantially better BLAST + [31] hits to a dataset of well-curated archaeal, bacterial and fungal genomes than to a metazoan database (both available from http://ryanlab.whitney. ufl.edu/downloads/alien_index/), defined as those exhibiting an alien index >45 (see [32]), were excluded. Sanitized transcriptomes were imported back into Agalma for orthology inference [28,33], which included tree-based steps to refine orthologues by identifying duplication events on gene trees and pruning putative paralogous sequences. Alignment and quality-based trimming were performed with MAFFT v. 7.305 [34] and GBLOCKS v. 0.91b [35]. The resulting supermatrix was reduced using a 70% occupancy threshold, resulting in a dataset composed of 1159 orthologues coded as amino acids (from a total of 13767).

Gene trees were inferred from each amino acid alignment with ParGenes v. 1.0.1 [36], using optimal models and 100 bootstrap replicates. These were analysed with TreeShrink v. 1.3.1 [37] (using parameters -q 0.01 -k 3 -b 25), which employs taxonspecific distributions of root-to-tip distances to identify outlier sequences potentially suffering from errors in alignment or orthology inference. Identified outliers were removed from both gene trees and individual alignments, and a new supermatrix was concatenated. As a final sanitation step, the data was run using genesortR [38,39], which ordered all loci based on decreasing estimates of phylogenetic usefulness (electronic supplementary material, figure S1). The worst-ranked 59 loci (5.1% of supermatrix) were further discarded, resulting in a final dataset of 1100 loci and 264 991 amino acid positions. Two smaller datasets, composed of the top-scoring (i.e. most phylogenetically useful) half and quarter of loci (550 and 225, respectively) were also output for analysis.

royalsocietypublishing.org/journal/rspb

Proc. R. Soc. B 290: 20230988

(c) Phylogenetic inference

Phylogenies were inferred from all three datasets using a variety of approaches. First, gene trees were provided to the coalescentaware summary method ASTRAL-III [40], which employs local posterior probabilities to estimate node support [41]. Second, tree inference was performed under a best-fit partitioned model with IQ-TREE 2 v. 2.1.3 [42-44], using the fast-relaxed clustering algorithm to merge individual loci (using parameters -m MFP + MERGE -rclusterf 10 -rcluster-max 3000). Finally, the site-heterogeneous model CAT-PMSF [45] was used as an efficient alternative to the computationally demanding CAT model family [46]. For each dataset, short runs of 1100 generations were done in PhyloBayes-MPI v. 1.8.1 [47] under a fixed topology (that obtained with ASTRAL-III) to approximate sitespecific stationary distributions and amino acid exchangeabilities under the CAT + GTR model. Model parameters were summarized after discarding the initial 100 generations as burn-in, and reformatted using scripts available at https://github.com/ drenal/cat-pmsf-paper. Tree inference was then performed in IQ-TREE 2 under maximum likelihood using the PMSF method [48], setting exchangeabilities and site-specific frequencies to the posterior mean estimates previously obtained with PhyloBayes. For both concatenation approaches, support was estimated using 1000 replicates of ultrafast bootstrap [49].

(d) Phylogenetic signal dissection

Several avenues were explored to assess levels of phylogenetic signal and conflict in the data. First, a treespace was built from gene trees using quartet dissimilarities to estimate topological differences and principal coordinate analysis (PCoA) as the method of ordination [50]. Levels of incongruence (henceforth, topological disparity) were compared between the complete and usefulness-based subsampled datasets using averaged Euclidean distances to the centroid. Values for subsampled datasets were then compared against null distributions built using 1000 replicates of randomly selected one half and one quarter of gene trees. This approach relied on R packages Quartet [51] and dispRity [52]. Loci were also characterized by their ability to recover several deep, well-supported and non-nested nodes: Apodida, Elasipodida, Holothuriida, Synallactida and Dendrochirotida (i.e. all currently recognized order-level clades [7] represented by at least three sampled terminals). Gene trees recovering a large proportion of 'uncontroversial' nodes have been considered less likely to suffer from hidden paralogy and more prone to retain true phylogenetic signals [53,54]. For each loci, results were summarized using the proportion of clades recovered from among those whose monophyly could be tested (i.e. those represented by at least two terminals).

Since there was persistent discordance among methods of inference regarding the resolution of major neoholothuriid clades, phylogenetic signal for the alternative topologies was explored using site-wise log-likelihood scores. Scores were computed with IQ-TREE 2 under the best-fit partitioned model and using three constrained topologies differing only in the position of Molpadida (the remaining incongruence was fixed to the preferred resolution, see Results). Gene-wise log-likelihood scores were obtained by adding scores across sites, and their differences for all pairs of topologies-known as AGLS values-were computed. Given linear dependency between the three ΔGLS values $(\Delta GLS_x = \Delta GLS_y - \Delta GLS_z)$, these were visualized in a two-dimensional space which was rotated using principal components analysis (PCA). A nominal ΔGLS threshold of ± 2 loglikelihood units was used to categorize loci as either informative or uninformative with regards to a given topological comparison. The relative enrichment for/against alternative neoholothuriid topologies was assessed in subsampled matrices enriched in both phylogenetic usefulness and loci recovering high proportions of 'uncontroversial' nodes (see above).

To explore the drivers of differences in ΔGLS across loci, fifteen gene properties were estimated and treated as potential determinants. These were all calculated by *genesortR* [39], and included commonly used metrics of phylogenetic signal, potential sources of systematic bias, and estimates of the overall information content and evolutionary rate of each individual loci. Further details on these metrics can be found in electronic supplementary material, table S2.

Potential links between gene properties and the phylogenetic support for alternative neoholothuriid relationships were explored using two different statistical approaches. Associations between the PCA axes derived from ΔGLS values (representing major aspects of phylogenetic signal for competing hypotheses) and explanatory variables were first tested using the 'envfit' function in R package vegan [55]. This approach overlayed vectors onto the ordination plot depicting the directions and magnitudes of maximum correlation between individual gene properties and PCA scores. Each predictor was analysed separately, and the significance of the correlations tested using 10 000 random permutations. Given the possibility of nonlinear relationships between predictor and response variables, a second approach was explored in which 4GLS values were transformed into a single categorical factor with three levels. For this, loci were categorized into: (A) uninformative, including those for which all ΔGLS were within ± 2 log-likelihood units; as well as those either (B) supporting or (C) rejecting the resolution obtained using ASTRAL-III, defined as exhibiting at least one comparison favouring or disfavouring such topology, respectively, by an absolute ΔGLS value >2. This categorization is supported by analyses showing that the main aspect of differences in phylogenetic signal across loci relates to their support for/against the topology obtained with ASTRAL-III, with very little ability to discriminate between the two other alternatives (see Results). A conditional inference classification tree was fit to the data using function 'ctree' in R package partykit [56], assessing whether partitioning the data by values of any of the gene properties was able to generate subsets of loci that show similar topological preferences. A Bonferroni correction for multiple comparisons was applied, and significant predictors were visualized on the ordination plot using smooth surfaces fit using penalized regression splines [57].

All statistical analyses were performed in the R environment v. 4.2.2 [58] using code reliant on the packages mentioned above, as well as *adephylo* [59], *ape* [60], *phangorn* [61], *phytools* [62] and those included in the *tidyverse* [63].

3. Results

Phylogenetic inference under all methods explored and for the three datasets of different sizes recovered highly congruent and well-supported topologies (electronic supplementary material, figures S2-S4), which were also in broad agreement with the most recent large-scale study based on Sangersequenced loci [16]. As summarized in figure 2a, Apodida, Elasipodida and Holothuriida formed successive and monophyletic sister groups to the remainder of sea cucumber diversity included within Neoholothuriida. The latter was further subdivided into four major lineages: Dendrochirotida, Molpadida, Persiculida and Synallactida. Nodes defining all aforementioned clades had maximum support across analyses. Support for currently recognized order level clades was surprisingly unambiguous: 69.2% of gene trees resolved a monophyletic Synallactida, and between 87.1 and 96.9% recovered the monophyly of Apodida, Elasipodida,

Figure 2. Summary of phylogenetic inference results. (*a*). Strict consensus of the nine inference conditions explored, varying both the number of loci and the method of inference. Nodes disagreeing between analyses are collapsed and labelled (see panels (*b,c*) for further details); branch lengths are otherwise taken from the CAT-PMSF analysis of the full dataset. (*b*). Monophyly of a clade composed of two cucumariid terminals, *Colochirus robustus* and *Cucumaria georgiana*, is rejected by ASTRAL-III, but upheld by the other methods (legend for support value grid is shown in (*a*)). (*c*). Systematic disagreement between all methods of inference regarding relationships among major neoholothuriid clades. The resolution favoured by each method is found across datasets of different sizes. Topologies, branch lengths and support values for each individual analysis are shown in electronic supplementary material, figures S2–S4.

Holothuriida and Dendrochirotida (electronic supplementary material, figure S5). Despite the relatively small size of loci (mean number of characters: 239.9, range = 103-621), 88.0% simultaneously resolved at least two thirds of these clades, and 58.1% resolved them all.

Downloaded from https://royalsocietypublishing.org/ on 01 April 2024

Only two regions of the tree topology showed incongruent resolutions among the analyses performed (figure 2b,c). First, ASTRAL-III rejected a close relationship among two of the cucumariid species sampled, Colochirus robustus and Cucumaria georgiana, which otherwise formed a clade under concatenation approaches (figure 2b). Given the otherwise unambiguous support for a close relationship between Colochirus and Cucumaria, as well as the poor node support for the ASTRAL-III topology when using the complete dataset, we tentatively favour here the results obtained under concatenation methods. We note, however, that a monophyletic Cucumariidae was not recovered by our analyses regardless of how these terminals are resolved, as they were only distantly related to the remaining cucumariids (Abyssocucumis, Pseudocolochirus). In fact, discrepancies between our trees and the current family level classification of sea cucumbers are pervasive, and also included the non-monophyly of elasipodid families Psychropotidae (Psychropotes, Benthodytes) and Laetmogonidae (Benthogone, Pannychia), the dendrochirotid family Sclerodactylidae (Cladolabes, Eupentacta, Sclerodactyla), and the synallactid families Synallactidae (Synallactes, Bathyplotes, Paelopatides) and Stichopodidae (Stichopus, Isostichopus, Apostichopus).

A second and more striking topological discordance involved the organization of the four major lineages within Neoholothuriida (figure 2c). Each one of the different methods of inference proposed an alternative resolution for the clade, which were recovered regardless of dataset size and strongly supported (values >95) when employing the complete supermatrix. While all three inference methods agreed on a subtree in which Dendrochirotida and Synallactida share a closer relationship than either one does with Persiculida, the position of Molpadida within this scaffold was highly unstable and methodologically sensitive. Supported alternatives included a placement of Molpadida as sister to either Synallactida, Persiculida, or Synallactida+ Dendrochirotida (henceforth referred to as 'ASTRAL', 'partitioned', and 'CAT-PMSF' topologies, respectively; figure 2c). Despite this level of uncertainty, our analyses still reject the long-hypothesized close relationships between Molpadida and Dendrochirotida [13,15], as well as the topology of Miller et al. [16] in which Dendrochirotida placed as sister group to all other neoholothuriids. While support values for some deep nodes decreased when performing inference with the smallest of datasets, this seems to be entirely driven by a reduction in the amount of data, as subsampled matrices showed significant reductions in overall phylogenetic conflict (estimated using topological disparity; electronic supplementary material, figure S6).

To further explore the phylogenetic signal for competing neoholothuriid topologies, we estimated gene-wise

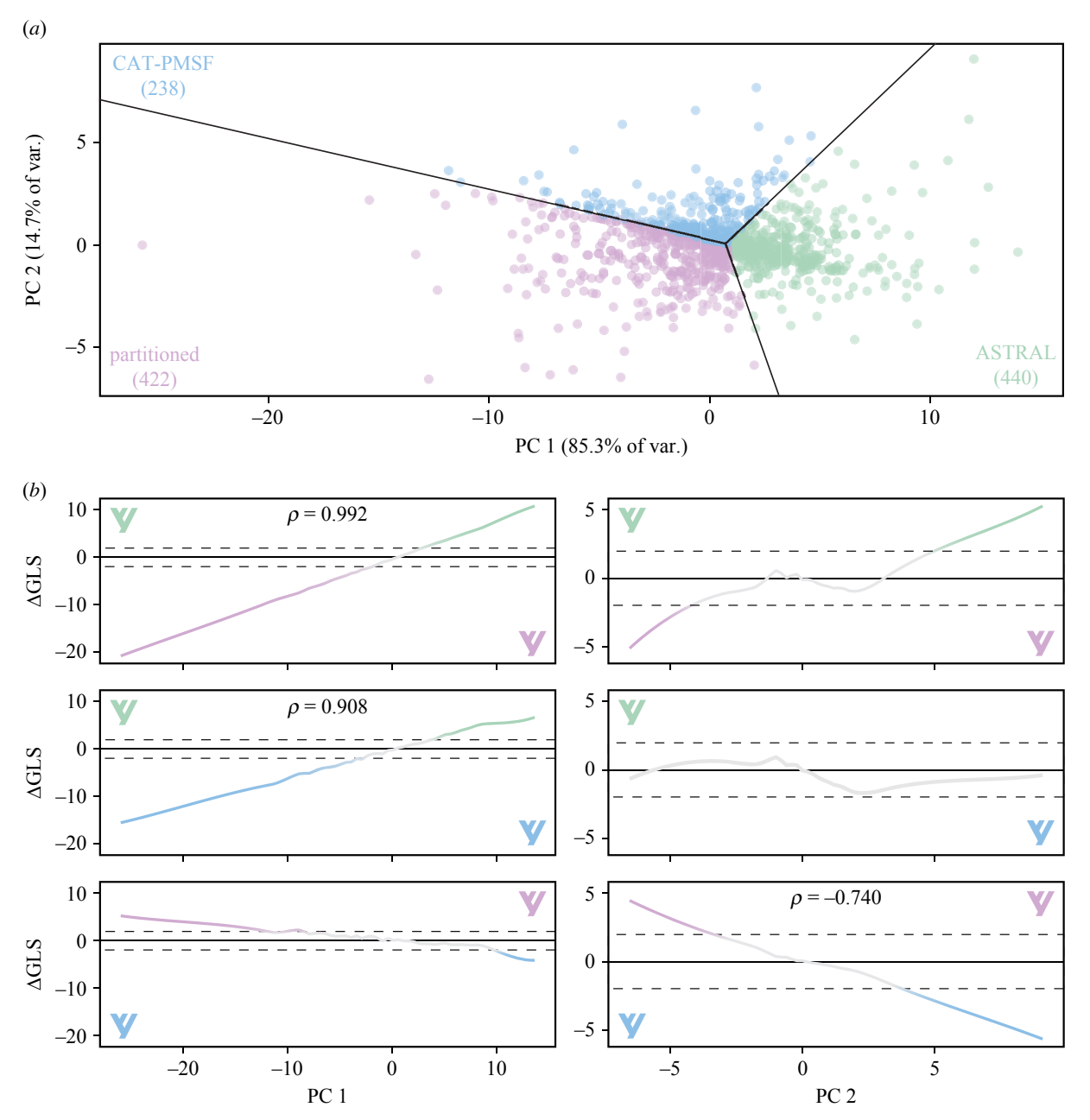


Figure 3. Exploration of support for alternative neoholothuriid topologies across loci. (a). Principal components (PC) axes obtained from the three Δ GLS. Percentages of explained variance are shown on axis labels. Loci are colour coded depending on their favoured topology. (b). Relationship between the PC axes and the scores of individual Δ GLS. Trendlines correspond to LOESS smoothing curves, and ρ -values (Spearman's rank correlation coefficients) are shown when absolute values > 0.7, taken to represent strong correlations. The area included within \pm 2 log-likelihood units is highlighted and considered an area of weak support. Note the markedly different scales of the γ -axes for PCs 1 and 2. Topologies are colour coded as in (a).

log-likelihood scores for the three alternative resolutions of this clade. A PCA of differences in the scores obtained for pairs of topologies (ΔGLS) revealed that the topological preferences of loci could be summarized using a single major underlying axis which accounted for 85.3% of total variance (figure 3a). The scores of loci along this first PC axis represented the relative support either for or against the ASTRAL topology (figure 3b). On the other hand, the ability of loci to discern between the partitioned and CAT-PMSF trees was much weaker and mainly captured by the second PC axis, which explained only 14.7% of variance. The absolute values of ΔGLS were generally small, with most loci (615 loci, 55.9% of the complete dataset) being relatively uninformative regarding relationships among neoholothuriid clades (figure 4a and electronic supplementary material, figure S7). Nonetheless, the remainder of the dataset was once again roughly evenly

split into a fraction that supported the ASTRAL configuration (207 loci, 18.8%), and one that rejected it in favour of either one, or both, of the topological alternatives (278 loci, 25.3%). These proportions remained stable across datasets subsampled using different strategies (electronic supplementary material, figure S8).

None of the 15 gene properties explored was recovered as a significant predictor of Δ GLS (figure 4b). Furthermore, these metrics correlated mostly with PC 2 (electronic supplementary material, table S2), leaving the major aspect of topological preference entirely unexplained. An alternative approach based on classification trees recovered one significant predictor: uninformative loci were significantly more likely to have a short alignment length, but this property also fails to explain which resolution was preferred by longer and more informative loci (electronic supplementary material, figure S9).

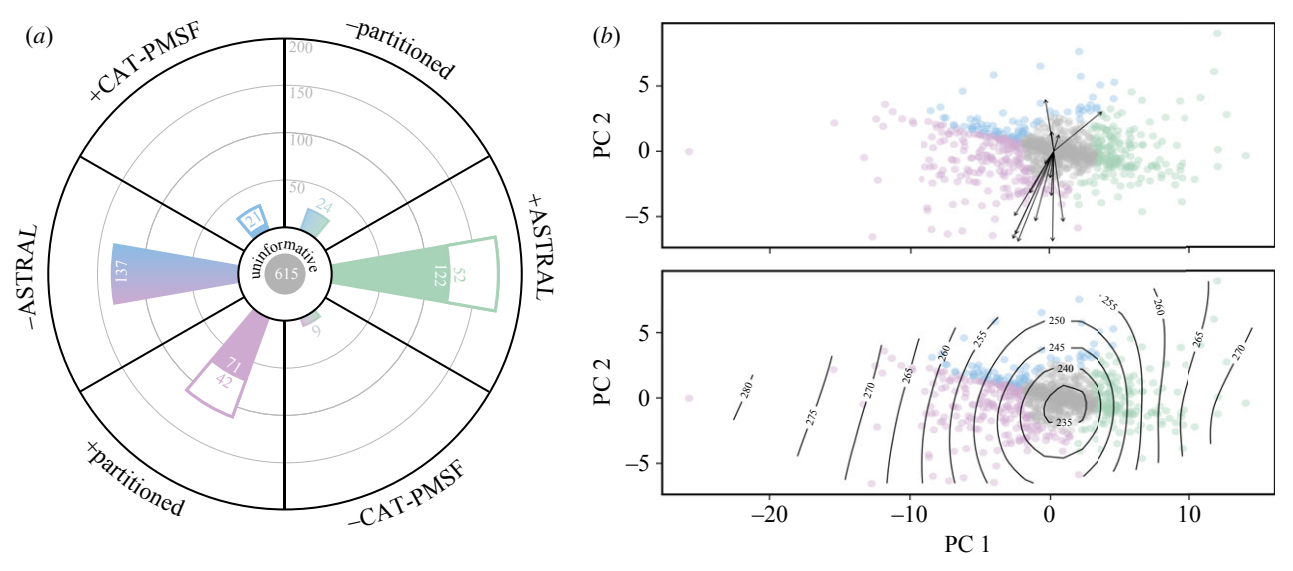


Figure 4. Categorization of loci depending on their favoured topology, and exploration of potential determinants. Colouring scheme follows that of figure 3. (*a*). Most loci (615, 55.9% of the full dataset) can be considered uninformative regarding relationships among neoholothuriid clades. The remainder can be classified into those supporting a given topology (denoted using a plus sign, +) if they favour a given resolution against both alternatives (coloured section of bar chart) or only one (white section of bar chart) with a Δ GLS ≥ 2; or rejecting a given topology (denoted using a minus sign, -). The number of loci either supporting (right side of wheel) or rejecting (left side of wheel) the ASTRAL topology are comparable in number: 207 (18.8%) versus 278 (25.3%), respectively. Further details on loci categorization can be found in electronic supplementary material, figure S7. (*b*). Top: Exploration of 15 potential determinants of Δ GLS. Arrows indicate directions of maximum correlation between scores and determinants; their length is scaled to the strength of the correlation. Predictors mostly load onto PC 2. R² and *p*-values are shown in electronic supplementary material, table S2, but no correlation is significant. Bottom: Smoothed surface of alignment length, the only significant determinant found using a classification tree. Longer loci are more likely to be informative, yet alignment length does not predict which topology is preferred (see electronic supplementary material, figure S9).

4. Discussion

Phylogenetic incongruence is a hallmark of genome-scale datasets [64-66]. A wide range of biological processes and methodological artefacts can lead phylogenomic datasets to harbour a mixture of phylogenetic signals, which can be differentially amplified by methods of reconstruction to produce conflicting, yet well-supported, topologies [67–69]. Different avenues have been proposed to ameliorate phylogenetic incongruence and favour a specific resolution for recalcitrant nodes. One strategy is to focus on data filtering, exploring the effects of removing sites and/or loci with unexpectedly high topological preferences [70,71], or those showing evidence of contributing mostly phylogenetic noise or biases [39,72]. Alternatively, methods have been developed to dissect alternative signals [73-75] in the hopes that one emerges as a better-justified option. Finally, exploring a range of inference methods, which vary in their realism, complexity, susceptibility to errors, and (potentially) relative fit, can also be used to justify favouring one among several alternative hypotheses [76-78]. However, even after exhaustive testing of these options, a robust resolution for some nodes on the tree of life remains elusive [79-82], awaiting the discovery of novel phylogenetic markers, improved taxon sampling or methodological developments.

We propose here that the early diversification of neoholothuriid sea cucumbers, an ancient, diverse and morphologically heterogeneous clade, constitutes another example of a group that defies phylogenetic resolution. Previous studies had acknowledged that a robust topology for Neoholothuriida was probably unattainable with the use of small molecular datasets [16], yet phylogenetic resolution remains out of reach even when employing more than a thousand loci. This result is particularly noteworthy given how comparatively trivial it is to

correctly reconstruct other deep nodes (electronic supplementary material, figure S5). The reason underlying this uncertainty is not a lack of statistical power, but the presence of multiple signals supporting alternative trees. While a node uniting Dendrochirotida and Synallactida to the exclusion of Persiculida emerges from all our analyses, the position of Molpadida within this topology remains uncertain. A coalescentaware method of reconstruction places Molpadida inside the clade containing Dendrochirotida and Synallactida, while concatenation-based methods place it outside, with further disagreement emerging depending on whether site-homogeneous or site-heterogeneous models are used. All three of these topological alternatives are well-supported and robust to gene subsampling, and thus represent an example of remarkable methodological sensitivity. Further exploration reveals that our dataset is unlikely to contain enough information to disambiguate between the topologies supported by alternative concatenation methods. On the other hand, the placements of Molpadida either inside or outside of the node containing Dendrochirotida + Synallactida are each strongly supported by substantial fractions of the data (19% and 25% of loci, respectively).

Complex site-heterogeneous models, such as the CAT family, are likely to fit genome-scale datasets better [48,83,84], but the use of model fit statistics when comparing mixture models against other alternatives (such as partitioned models) has been criticized [85]. Furthermore, issues relating to convergence, missing data, and over-parameterization [86–88] have still led many to question the results obtained under CAT models. Similarly, coalescent-aware methods have outperformed concatenation in a number of simulation scenarios [89,90], yet doubts remain regarding their usefulness to resolve ancient divergences, given that gene tree error is expected to surpass incomplete lineage

sorting as the dominant source of incongruence for deep nodes [91]. The fit of summary methods (such as ASTRAL) is also impossible to evaluate relative to that of others, further complicating arriving at an objective way of preferring one method of inference from among those tested here.

In the absence of clear guidance as to which inference method should be preferred, we focused instead on evaluating the amount and quality of the signals supporting alternative placements of Molpadida. We used ΔGLS as proxies for the topological preference of loci (as in e.g. [19,70,92]), extending this type of analysis to simultaneously consider three alternative topologies. This allowed us to uncover a strong asymmetry in the ability of loci to distinguish between alternative trees and, as explained above, redirect our efforts to assessing two broad topological alternatives. Although many studies have succeeded in disentangling phylogenetic from non-phylogenetic signals by exploring loci quality [93-95], our attempts failed to find any determinants of topological preference: loci supporting alternative positions of Molpadida do not differ in their levels of phylogenetic signal, systematic biases, amounts of information or evolutionary rates. The only major pattern uncovered is that longer loci are more likely to harbour some sort of signal, a predictable and relatively trivial result stemming from the increased statistical power of longer alignments.

The branches subtending the major neoholothuriid clades are remarkably short (electronic supplementary material, figures S2-S4). This scenario, coupled with the deep origin of the major clades of crown holothuroids [16,96], is expected to result in unfavourable signal to noise ratios [97]. Nonetheless, the finding that substantial fractions of our supermatrix exhibit strong signal for competing topologies is not in line with Neoholothuriida originating from a hard polytomy [98]. Two broad explanations are therefore consistent with our results. First, incongruence might be caused by types of model violations that were not explicitly tested here, as would result, for example, from convergent shifts in amino acid composition [98-100]. Alternatively, neoholothuriid evolution might be better explained by ancient events of reticulation, as produced by processes such as ancient hybridization and incomplete lineage sorting. Finding direct evidence to substantiate these claims is complicated by the relatively sparse sampling attained by this study, the limited genomic resources available for the clade, and the lack of available methods that can simultaneously address both of these processes [79]. We suggest that Neoholothuriida constitutes a case of an ancient and rapid radiation, and further progress in its resolution could benefit from targeting data whose evolutionary history proves easier to model. Addressing the currently sparse sampling of both Molpadida and Persiculida should also be prioritized if we are to resolve this lingering uncertainty, especially through the sequencing of morphologically unique and potentially deeply divergent lineages such as Caudinidae, Eupyrigidae and Gephyrothuriidae.

Although the exact placement of Molpadida remains challenging to ascertain, phylogenomics reveals an otherwise robust higher-level topology for sea cucumbers. These efforts are a major step towards a stable classification for the group, corroborating much of the most recent classification based on a small-scale molecular dataset [16]. The results presented here constitute a necessary tool with which to elucidate the times of origin, morphological evolution and diversification dynamics of a major lineage of marine invertebrates. At the same time, they also show the extent to which the current family level classification scheme of holothuroids is at odds with their evolutionary history, highlighting the need for phylogenomic investigations with much-expanded taxon sampling and consequent morphological reassessments.

Ethics. Specimen collection and fieldwork in Costa Rica were performed under permits R-070-2018-OTCONAGEBIO issued by CONAGEBIO (Comisión Nacional para la Gestión de la Biodiversidad) and INCOPESCA-CPI-003-12-2018 issued by INCOPESCA (Instituto Costarricense de Pesca y Acuicultura).

Data accessibility. COI sequences are available from GenBank under accession numbers OR082743-OR082756 and OR145350-OR145353; transcriptomic raw reads are available from SRA under BioProject PRJNA979278. All assemblies, phylogenomic datasets and trees, and other results, can be obtained from the Dryad Digital Repository: https://doi.org/10.5061/dryad.0p2ngf255 [26].

Supplementary figures and tables are provided in the electronic supplementary material [101].

Authors' contributions. N.M.K.: conceptualization, data curation, formal analysis, funding acquisition, investigation, methodology, software, visualization, writing—original draft, writing—review and editing; E.T.: data curation, writing—review and editing; A.K.M.: conceptualization, writing—review and editing; J.S.: data curation, writing—review and editing; G.W.R.: conceptualization, funding acquisition, project administration, resources, writing—original draft, writing—review and editing.

All authors gave final approval for publication and agreed to be held accountable for the work performed therein.

Conflict of interest declaration. We declare we have no competing interests. Funding. This work was supported by the Schmidt Ocean Institute, The David and Lucille Packard Foundation, University of California Ship Funds, the US National Science Foundation (NSF) Division of Environmental Biology (DEB) grants DEB-1036368 and DEB-2036186, and the NSF Office of Polar Programs grant OPP-1043749. Open Access was made available through support from the University of California Libraries and the Schmidt Ocean Institute.

Acknowledgements. Many thanks to Bob Vrijenhoek and David Clague of the Monterey Bay Aquarium Research Institute and the captain and crew of the R/V Western Flyer for sampling opportunities. Thanks also to the Schmidt Ocean Institute and chief scientists, Erik Cordes, Pete Girguis and Lisa Levin, and science parties of the R/V Falkor cruises FK181005, FK190106 and FK210726. We are also grateful to the captain and crew of the R/V Robert Gordon Sproul and the R/V IB Nathaniel B. Palmer and science participants during the cruise NBP-1303. Many thanks to the pilots of the remote operated vehicles Doc Ricketts and SuBastian for crucial assistance in specimen collection. We also thank Avery Hiley and Marina McCowin for assistance in the laboratory and to Charlotte Seid (SIO-BIC) for specimen cataloguing. This manuscript was improved by comments from Gary Carvalho, Ricardo Betancur-R and two anonymous reviewers. The beginning of the title is taken from the 1969 song 'Epitaph' by King Crimson.

References

Downloaded from https://royalsocietypublishing.org/ on 01 April 2024

- Becher S. 1906 Über Synapta minuta n. sp., eine brutpflegende Synaptide der Nordsee, und über die contractilen Rosetten der Holothurien. Zool. Anz. 30, 505–509.
- O'Loughlin PM, O'Hara TD. 1992 New cucumariid holothurians (Echinodermata) from southern Australia, including two brooding and one fissiparous species. Mem.
- *Mus. Vic.* **53**, 227–266. (doi:10.24199/j.mmv. 1992.53.12)
- Flammang P, Conand C. 2004 Functional morphology of the tentacles in the apodid holothuroid Synapta

- maculata. In Echinoderms: München proceedings of the 11th International Echinoderm Conference, Munich, Germany, pp. 327–333. London, IIK: CRC Press
- Purcell SW, Samyn Y, Conand C. 2012 Commercially important sea cucumbers of the world. Rome, Italy: FAO
- Selig GM, Netburn AN, Malik M. 2019 Distributions of the pelagic holothurian Pelagothuria in the central Pacific Ocean as observed by remotelyoperated vehicle surveys. Front. Mar. Sci. 6, 684. (doi:10.3389/fmars.2019.00684)
- O'Hara T, Byrne M. 2017 Australian echinoderms: biology, ecology and evolution. Victoria, Australia: CSIRO Publishing.
- WoRMS Editorial Board. 2022 World register of marine species. See https://www. marinespecies.org
- Gallo ND, Cameron J, Hardy K, Fryer P, Bartlett DH, Levin LA. 2015 Submersible-and lander-observed community patterns in the Mariana and New Britain trenches: influence of productivity and depth on epibenthic and scavenging communities. *Deep* Sea Res. Part 1 99, 119–133. (doi:10.1016/j.dsr. 2014.12.012)
- Souza Junior J, Ponte I, Melo Coe C, Lobo Farias WR, Vieira Feitosa C, Hamel JF, & Mercier A. 2017 Sea cucumber fisheries in Northeast Brazil. SPC Beche-de-mer Information Bulletin 37, 43–47.
- Belyaev G. 1972 Hadal bottom fauna of the world ocean. Jerusalem, Israel: Israel Program for Scientific Translations.
- Slater M, Chen J. 2015 Sea cucumber biology and ecology. In *Echinoderm aquaculture* (eds NP Brown, SD Eddy), pp. 47–56. Hoboken, NJ: Wiley-Blackwell.
- 12. Billett D. 1988 *The ecology of deep-sea holothurians*. Southampton, UK: University of Southampton.
- Smirnov A. 2012 System of the class Holothuroidea. *Paleontol. J.* 46, 793–832. (doi:10.1134/ S0031030112080126)
- Smirnov A. 2016 Parallelisms in the evolution of sea cucumbers (Echinodermata: Holothuroidea).
 Paleontol. J. 50, 1610–1625. (doi:10.1134/ S0031030116140082)
- Kerr AM, Kim J. 2001 Phylogeny of Holothuroidea (Echinodermata) inferred from morphology.
 Zool. J. Linn. Soc. 133, 63–81. (doi:10.1111/j.1096-3642.2001.tb00623.x)
- Miller AK, Kerr AM, Paulay G, Reich M, Wilson NG, Carvajal JI, Rouse GW. 2017 Molecular phylogeny of extant Holothuroidea (Echinodermata). *Mol. Phylogenet. Evol.* 111, 110–131. (doi:10.1016/j. ympev.2017.02.014)
- Brown WI, Shick JM. 1979 Bimodal gas exchange and the regulation of oxygen uptake in holothurians. *Biol. Bull.* 156, 272–288. (doi:10. 2307/1540917)
- Jaeckle WB, Strathmann RR. 2013 The anus as a second mouth: anal suspension feeding by an oral deposit-feeding sea cucumber. *Invertebr. Biol.* 132, 62–68. (doi:10.1111/ivb.12009)
- Mongiardino Koch N, Coppard SE, Lessios HA, Briggs DE, Mooi R, Rouse GW. 2018 A phylogenomic

- resolution of the sea urchin tree of life. *BMC Evol. Biol.* **18**, 189. (doi:10.1186/s12862-018-1300-4)
- Linchangco Jr GV et al. 2017 The phylogeny of extant starfish (Asteroidea: Echinodermata) including *Xyloplax*, based on comparative transcriptomics. *Mol. Phylogenet. Evol.* 115, 161–170. (doi:10.1016/j.ympev.2017.07.022)
- O'Hara TD, Hugall AF, Thuy B, Moussalli A. 2014 Phylogenomic resolution of the class Ophiuroidea unlocks a global microfossil record. *Curr. Biol.* 24, 1874–1879. (doi:10.1016/j.cub.2014.06.060)
- Janies DA, Witter Z, Linchangco GV, Foltz DW, Miller AK, Kerr AM, Jay J, Reid RW, Wray GA. 2016 EchinoDB, an application for comparative transcriptomics of deeply-sampled clades of echinoderms. *BMC Bioinf*. 17, 48. (doi:10.1186/ s12859-016-0883-2)
- Clouse RM, Linchangco Jr GV, Kerr AM, Reid RW, Janies DA. 2015 Phylotranscriptomic analysis uncovers a wealth of tissue inhibitor of metalloproteinases variants in echinoderms. R. Soc. Open Sci. 2, 150377. (doi:10.1098/rsos.150377)
- 24. Faircloth BC, Glenn TC. 2012 Not all sequence tags are created equal: designing and validating sequence identification tags robust to indels. *PLoS ONE* **7**, e42543. (doi:10.1371/journal.pone.0042543)
- Kudtarkar P, Cameron RA. 2017 Echinobase: an expanding resource for echinoderm genomic information. *Database* 2017, bax074. (doi:10.1093/ database/bax074)
- Mongiardino Koch N, Tilic E, Miller AK, Stiller J, Rouse GW. 2023 Data from: Confusion will be my epitaph: genome-scale discordance stifles phylogenetic resolution of Holothuroidea. Dryad Digital Repository. (doi:10.5061/dryad.0p2ngf255)
- Bolger AM, Lohse M, Usadel B. 2014 Trimmomatic: a flexible trimmer for Illumina sequence data. *Bioinformatics* 30, 2114–2120. (doi:10.1093/bioinformatics/btu170)
- Dunn CW, Howison M, Zapata F. 2013 Agalma: an automated phylogenomics workflow. *BMC Bioinf*.
 14, 330. (doi:10.1186/1471-2105-14-330)
- Grabherr MG et al. 2011 Full-length transcriptome assembly from RNA-Seq data without a reference genome. Nat. Biotechnol. 29, 644–652. (doi:10. 1038/nbt.1883)
- Ryan JF. 2014 Alien Index: identify potential nonanimal transcripts or horizontally transferred genes in animal transcriptomes. (doi:10.5281/zenodo. 21029)
- Camacho C, Coulouris G, Avagyan V, Ma N, Papadopoulos J, Bealer K, Madden TL. 2009 BLAST+: architecture and applications. *BMC Bioinf*. 10, 421. (doi:10.1186/1471-2105-10-421)
- 32. Gladyshev EA, Meselson M, Arkhipova IR. 2008

 Massive horizontal gene transfer in bdelloid rotifers. *Science* 320, 1210–1213. (doi:10.1126/science.
- Guang A, Howison M, Zapata F, Lawrence CE, Dunn
 C. 2017 Revising transcriptome assemblies with phylogenetic information. *PLoS ONE* 16, e0244202.
- 34. Katoh K, Standley DM. 2013 MAFFT multiple sequence alignment software version 7:

- improvements in performance and usability. *Mol. Biol. Evol.* **30**, 772–780. (doi:10.1093/molbev/mst010)
- Talavera G, Castresana J. 2007 Improvement of phylogenies after removing divergent and ambiguously aligned blocks from protein sequence alignments. Syst. Biol. 56, 564–577. (doi:10.1080/ 10635150701472164)
- Morel B, Kozlov AM, Stamatakis A. 2018 ParGenes: a tool for massively parallel model selection and phylogenetic tree inference on thousands of genes. *Bioinformatics* 35, 1771–1773. (doi:10.1093/ bioinformatics/bty839)
- Mai U, Mirarab S. 2018 TreeShrink: fast and accurate detection of outlier long branches in collections of phylogenetic trees. *BMC Genom.* 19, 272. (doi:10. 1186/s12864-018-4620-2)
- 38. Mongiardino Koch N, Thompson JR. 2021 A totalevidence dated phylogeny of Echinoidea combining phylogenomic and paleontological data. *Syst. Biol.* **70**, 421–439. (doi:10.1093/sysbio/syaa069)
- Mongiardino Koch N. 2021 Phylogenomic subsampling and the search for phylogenetically reliable loci. *Mol. Biol. Evol.* 38, 4025–4038. (doi:10. 1093/molbev/msab151)
- Zhang C, Rabiee M, Sayyari E, Mirarab S. 2018
 ASTRAL-III: polynomial time species tree
 reconstruction from partially resolved gene trees.
 BMC Bioinf. 19, 153. (doi:10.1186/s12859-018 2129-y)
- Sayyari E, Mirarab S. 2016 Fast coalescent-based computation of local branch support from quartet frequencies. *Mol. Biol. Evol.* 33, 1654–1668. (doi:10. 1093/molbev/msw079)
- Minh BQ, Schmidt HA, Chernomor O, Schrempf D, Woodhams MD, Von Haeseler A, Lanfear R. 2020 IQ-TREE 2: new models and efficient methods for phylogenetic inference in the genomic era. *Mol. Biol. Evol.* 37, 1530–1534. (doi:10.1093/molbev/msaa015)
- Kalyaanamoorthy S, Minh BQ, Wong TK, von Haeseler A, Jermiin LS. 2017 ModelFinder: fast model selection for accurate phylogenetic estimates. Nat. Methods 14, 587. (doi:10.1038/nmeth.4285)
- 44. Chernomor O, von Haeseler A, Minh BQ. 2016
 Terrace aware data structure for phylogenomic inference from supermatrices. *Syst. Biol.* **65**, 997–1008. (doi:10.1093/sysbio/syw037)
- Szánthó LL, Lartillot N, Szöllősi GJ, Schrempf D. 2023 Compositionally constrained sites drive long branch attraction. Syst. Biol., syad013. (doi:10.1093/ sysbio/syad013)
- Lartillot N, Philippe H. 2004 A Bayesian mixture model for across-site heterogeneities in the aminoacid replacement process. *Mol. Biol. Evol.* 21, 1095–1109. (doi:10.1093/molbev/msh112)
- Lartillot N, Rodrigue N, Stubbs D, Richer J. 2013 PhyloBayes MPI. Phylogenetic reconstruction with infinite mixtures of profiles in a parallel environment. Syst. Biol. 62, 611–615. (doi:10.1093/ sysbio/syt022)
- 48. Wang HC, Minh BQ, Susko E, Roger AJ. 2018 Modeling site heterogeneity with posterior mean

- site frequency profiles accelerates accurate phylogenomic estimation. Syst. Biol. 67, 216-235. (doi:10.1093/sysbio/syx068)
- 49. Hoang DT, Chernomor O, Von Haeseler A, Minh BQ, Vinh LS. 2018 UFBoot2: improving the ultrafast bootstrap approximation. Mol. Biol. Evol. 35, 518-522. (doi:10.1093/molbev/msx281)
- 50. Smith MR. 2022 Robust analysis of phylogenetic tree space. Syst. Biol. 71, 1255-1270. (doi:10.1093/ sysbio/syab100)
- 51. Smith MR. 2019 Quartet: comparison of phylogenetic trees using quartet and split measures. R package version 1.2.4. See https:// ms609.github.io/Quartet/.
- 52. Guillerme T. 2018 dispRity: A modular R package for measuring disparity. Methods Ecol. Evol. 97, 1755-1763. (doi:10.1111/2041-210X.13022)
- 53. Siu-Ting K, Torres-Sánchez M, San Mauro D, Wilcockson D. Wilkinson M. Pisani D. O'Connell MJ. Creevey DJ. 2019 Inadvertent paralog inclusion drives artifactual topologies and timetree estimates in phylogenomics. Mol. Biol. Evol. 36, 1344-1356. (doi:10.1093/molbev/msz067)
- 54. Hervé P et al. 2019 Mitigating anticipated effects of systematic errors supports sister-group relationship between Xenacoelomorpha and Ambulacraria. Curr. Biol. 29, 1818-1826. (doi:10.1016/j.cub.2019.04.009)
- 55. Oksanen J et al. 2019 vegan: community ecology package. R package version 2.5-4. https://CRAN.Rproject.org/package=vegan
- 56. Hothorn T, Zeileis A. 2015 partykit: a modular toolkit for recursive partytioning in R. J. Mach. Learn. Res. 16, 3905-3909.

Downloaded from https://royalsocietypublishing.org/ on 01 April 2024

- 57. Wood SN. 2003 Thin plate regression splines. J. R. Stat. Soc.: B (Stat. Methodol.) 65, 95-114. (doi:10.1111/1467-9868.00374)
- 58. Core Team R. 2019 R: a language and environment for statistical computing. Vienna, Austria: R Foundation for Statistical Computing.
- 59. Jombart T, Dray S. 2010 adephylo: exploratory analyses for the phylogenetic comparative method. Bioinformatics 26, 1-21. (doi:10.1093/ bioinformatics/btq292)
- Paradis E, Schliep K. 2018 ape 5.0: an environment for modern phylogenetics and evolutionary analyses in R. Bioinformatics 35, 526-528. (doi:10.1093/ bioinformatics/bty633)
- 61. Schliep KP. 2011 phangorn: phylogenetic analysis in R. Bioinformatics 27, 592-593. (doi:10.1093/ bioinformatics/btg706)
- 62. Revell LJ. 2012 phytools: an R package for phylogenetic comparative biology (and other things). Methods Ecol. Evol. 3, 217–223. (doi:10. 1111/j.2041-210X.2011.00169.x)
- 63. Wickham H. 2017 tidyverse: easily install and load 'tidyverse' packages. R package version 1.2.1. See https://CRAN.R-project.org/package=tidyverse
- 64. Mongiardino Koch N. 2019 The phylogenomic revolution and its conceptual innovations: a text mining approach. Org. Div. Evol. 19, 99-103. (doi:10.1007/s13127-019-00397-0)
- Jeffroy O, Brinkmann H, Delsuc F, Philippe H. 2006 Phylogenomics: the beginning of incongruence?

- Trends Genet. 22, 225-231. (doi:10.1016/j.tig.2006. 02.003)
- 66. Lozano-Fernandez J. 2022 A practical guide to design and assess a phylogenomic study. Genome Biol. Evol. 14, evac129. (doi:10.1093/gbe/evac129)
- 67. Delsuc F, Brinkmann H, Philippe H. 2005 Phylogenomics and the reconstruction of the tree of life. Nat. Rev. Genet. 6, 361-375. (doi:10.1038/ nrg1603)
- 68. Kapli P, Yang Z, Telford MJ. 2020 Phylogenetic tree building in the genomic age. Nat. Rev. Genet. 21, 428-444. (doi:10.1038/s41576-020-0233-0)
- 69. Philippe H, Brinkmann H, Lavrov DV, Littlewood DTJ, Manuel M, Wörheide G, Baurain D. 2011 Resolving difficult phylogenetic questions: why more sequences are not enough. PLoS Biol. 9, e1000602. (doi:10.1371/journal.pbio.1000602)
- 70. Shen X-X, Hittinger CT, Rokas A. 2017 Contentious relationships in phylogenomic studies can be driven by a handful of genes. Nat. Ecol. Evol. 1, 0126. (doi:10.1038/s41559-017-0126)
- 71. Francis WR, Canfield DE. 2020 Very few sites can reshape the inferred phylogenetic tree. PeerJ 8, e8865. (doi:10.7717/peerj.8865)
- 72. Dornburg A, Su Z, Townsend JP. 2019 Optimal rates for phylogenetic inference and experimental design in the era of genome-scale data sets. Syst. Biol. 68, 145-156. (doi:10.1093/sysbio/syy047)
- 73. Arcila D et al. 2017 Genome-wide interrogation advances resolution of recalcitrant groups in the tree of life. Nat. Ecol. Evol. 1, 0020. (doi:10.1038/ s41559-016-0020)
- 74. Smith SA, Walker-Hale N, Walker JF, Brown JW. 2020 Phylogenetic conflicts, combinability, and deep phylogenomics in plants. Syst. Biol. 69, 579-592. (doi:10.1093/sysbio/syz078)
- 75. Walker JF, Smith SA, Hodel RG, Moyroud E. 2022 Concordance-based approaches for the inference of relationships and molecular rates with phylogenomic data sets. Syst. Biol. 71, 943-958. (doi:10.1093/sysbio/syab052)
- 76. Feuda R, Dohrmann M, Pett W, Philippe H, Rota-Stabelli O, Lartillot N, Wörheide G, Pisani D. 2017 Improved modeling of compositional heterogeneity supports sponges as sister to all other animals. Curr. Biol. 27, 3864-3870. (doi:10.1016/j.cub.2017.11.008)
- 77. Song S, Liu L, Edwards SV, Wu S. 2012 Resolving conflict in eutherian mammal phylogeny using phylogenomics and the multispecies coalescent model. Proc. Natl Acad. Sci. USA 109, 14 942-14 947. (doi:10.1073/pnas.1211733109)
- 78. Redmond AK, McLysaght A. 2021 Evidence for sponges as sister to all other animals from partitioned phylogenomics with mixture models and recoding. Nat. Commun. 12, 1-14. (doi:10. 1038/s41467-021-22074-7)
- 79. Cunha TJ, Reimer JD, Giribet G. 2022 Investigating sources of conflict in deep phylogenomics of vetigastropod snails. Syst. Biol. 71, 1009-1022. (doi:10.1093/sysbio/syab071)
- King N, Rokas A. 2017 Embracing uncertainty in reconstructing early animal evolution. Curr. Biol. 27, R1081-R1088. (doi:10.1016/j.cub.2017.08.054)

- 81. Simon S, Blanke A, Meusemann K. 2018 Reanalyzing the Palaeoptera problem: the origin of insect flight remains obscure. Arthropod. Struct. Dev. 47, 328-338. (doi:10.1016/j.asd.2018.05.002)
- 82. Ontano AZ et al. 2021 Taxonomic sampling and rare genomic changes overcome long-branch attraction in the phylogenetic placement of pseudoscorpions. Mol. Biol. Evol. 38, 2446-2467. (doi:10.1093/ molbev/msab038)
- 83. Si Quang L, Gascuel O, & Lartillot N. 2008 Empirical profile mixture models for phylogenetic reconstruction. Bioinformatics 24, 2317-2323. (doi:10.1093/bioinformatics/btn445)
- 84. Schrempf D, Lartillot N, Szöllősi G. 2020 Scalable empirical mixture models that account for acrosssite compositional heterogeneity. Mol. Biol. Evol. **37**, 3616–3631. (doi:10.1093/molbev/msaa145)
- 85. Crotty SM, Holland BR. 2022 Comparing partitioned models to mixture models: do information criteria apply? Syst. Biol. 71, 1541-1548. (doi:10.1093/ sysbio/syac003)
- 86. Whelan NV, Halanych KM. 2016 Who let the CAT out of the bag? Accurately dealing with substitutional heterogeneity in phylogenomic analyses. Syst. Biol. 66, 232-255.
- Li Y, Shen X-X, Evans B, Dunn CW, Rokas A. 2021 Rooting the animal tree of life. Mol. Biol. Evol. 38, 4322-4333. (doi:10.1093/molbev/msab170)
- Al Jewari C, Baldauf SL. 2022 Conflict over the eukaryote root resides in strong outliers, mosaics and missing data sensitivity of site-specific (CAT) mixture models. Syst. Biol. 72, 1-6. (doi:10.1093/ sysbio/syac029)
- Kubatko LS, Degnan JH. 2007 Inconsistency of phylogenetic estimates from concatenated data under coalescence. Syst. Biol. 56, 17-24. (doi:10. 1080/10635150601146041)
- 90. Mirarab S, Bayzid MS, Warnow T. 2016 Evaluating summary methods for multilocus species tree estimation in the presence of incomplete lineage sorting. Syst. Biol. 65, 366-380. (doi:10.1093/sysbio/syu063)
- 91. Gatesy J, Springer MS. 2014 Phylogenetic analysis at deep timescales: unreliable gene trees, bypassed hidden support, and the coalescence/ concatalescence conundrum. Mol. Phylogenet. Evol. **80**, 231–266. (doi:10.1016/j.ympev.2014.08.013)
- Ballesteros JA, Sharma PP. 2019 A critical appraisal of the placement of Xiphosura (Chelicerata) with an account of known sources of phylogenetic error. Syst. Biol. 68, 896-917. (doi:10.1093/sysbio/syz011)
- Ballesteros JA et al. 2022 Comprehensive species sampling and sophisticated algorithmic approaches refute the monophyly of Arachnida. Mol. Biol. Evol. 39, msac021. (doi:10.1093/molbev/msac021)
- Burbrink FT et al. 2020 Interrogating genomic-scale data for Squamata (lizards, snakes, and amphisbaenians) shows no support for key traditional morphological relationships. Syst. Biol. 69, 502-520. (doi:10.1093/sysbio/syz062)
- Smith BT et al. 2022 Phylogenomic analysis of the parrots of the world distinguishes artifactual from biological sources of gene tree discordance. Syst. Biol. 72, 228-241. (doi:10.1093/sysbio/syac055)

- Mongiardino Koch N et al. 2022 Phylogenomic analyses of echinoid diversification prompt a reevaluation of their fossil record. Elife 11, e72460. (doi:10.7554/eLife.72460)
- 97. Townsend JP, Su Z, Tekle YI. 2012
 Phylogenetic signal and noise: predicting
 the power of a data set to resolve phylogeny.

 Syst. Biol. 61, 835–849. (doi:10.1093/
 sysbio/sys036)

Downloaded from https://royalsocietypublishing.org/ on 01 April 2024

- 98. Reddy S *et al.* 2017 Why do phylogenomic data sets yield conflicting trees? Data type influences the avian tree of life more than taxon sampling. *Syst. Biol.* **66**, 857–879. (doi:10.1093/sysbio/syx041)
- Rota-Stabelli O, Lartillot N, Philippe H, Pisani D. 2013
 Serine codon-usage bias in deep phylogenomics:
 Pancrustacean relationships as a case study. Syst. Biol.
 62, 121–133. (doi:10.1093/sysbio/sys077)
- Pandey A, Braun EL. 2020 Phylogenetic analyses of sites in different protein structural environments result in distinct placements of the metazoan root. *Biology* 9, 64. (doi:10.3390/biology9040064)
- 101. Mongiardino Koch N, Tilic E, Miller AK, Stiller J, Rouse GW. 2023 Confusion will be my epitaph: genome-scale discordance stifles phylogenetic resolution of Holothuroidea. Figshare. (doi:10.6084/ m9.figshare.c.6707571)